

Navier–Stokes computations Applied to tilt-rotors

Julien Decours ¹, Thierry Lefebvre ²

1 Applied Aerodynamics Department
ONERA, BP 72, 92322 Châtillon Cedex, France
e-mail: julien.decours@onera.fr

2 Applied Aerodynamics Department
ONERA, BP 72, 92322 Châtillon Cedex, France
e-mail: thierry.lefebvre@onera.fr

Key words: Tilt-rotor, Performance, Numerical simulation, Aerodynamic interaction, Rotor

Abstract: *A tilt-rotor is an aircraft which can combine both advantages of the good hovering capability of helicopters and the high speed cruise possibilities of conventional airplanes thanks to the conversion of its nacelles. But this requires controlling the aerodynamic interactions between the rotor, the nacelle and the wings in addition to the rotor performance from hover to cruise mode. Those themes have been studied in the frame of European programs including experimental test in the DNW-LLF wind tunnel and Navier-Stokes simulations performed by ONERA with the elsA software. Finally this paper constitutes a status on the ONERA knowledge about tilt-rotor aerodynamic interactions and rotor performance optimization.*

INTRODUCTION

A tilt-rotor is an aircraft which can combine both advantages of the good hovering capacity of helicopters and the high speed cruise possibilities of conventional airplanes thanks to the conversion of its nacelles, from the hover position (in helicopter mode) to the cruise position (in propeller mode). Thus, the development of the tilt-rotor technology is very attractive and it is important to understand aerodynamic performance and interactions between the different components. Therefore, the European Union decided to launch several research programs funded within the framework of the 5th PCRD that aim at developing a new generation of tilt-rotors in Europe, based on the ERICA (Figure 1) half moveable wing concept proposed by AGUSTA [1].

The conversion corridor is the critical tilt-rotor flight phase which lies on between the helicopter hover mode and the airplane level flight mode. Thus, it is very important to understand the aerodynamic interactions between the wings, the nacelle and the rotor in order to improve the aircraft performance and stability. Therefore the TILTAERO test campaign were covered a wide range of the flight envelope. In particular six reference test points have been chosen in the conversion corridor to be tested on a half-span 40% Mach-scaled model based on the advanced European tilt-rotor concept ERICA. Those configurations were tested in the DNW-LLF wind tunnel and also simulated by Navier-Stokes computations performed with the ONERA *elsA* software. Comparisons between experimental and numerical results have been done in order to understand the aerodynamic interactions during the tilt-rotor conversion.

The tilt-rotor blades also appear as a critical part of the aircraft because it has to compromise helicopter hover capability and manoeuvrability with aircraft cruise performance, within a restricted environmental context. Therefore in the frame of the ADYN and DART European projects, ONERA was responsible for the aerodynamics and acoustics optimizations of a new rotor dedicated

to the ERICA concept. The purpose of this task was to experimentally evaluate the ERICA reference blades (TILTAERO blades) in terms of noise characteristics and to perform a numerical optimization of a new set of blades (ADYN blades), which were designed, manufactured and tested in the same conditions. The optimization process and the experimental test of both rotors in terms of noise and performance are detailed in the following study.

The mock-up experimental setting and the DNW wind tunnel tests are described in the first part of the paper. Then, details on CFD numerical methods are given in the second part of the paper, followed by detailed comparisons between experimental measurement and numerical predictions of the conversion corridor configurations. Finally we focus on rotor performance simulations and optimization.

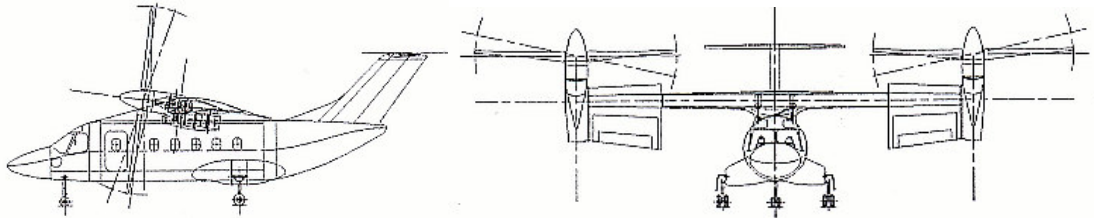


Figure 1: The ERICA tilt-rotor

1. TILT-ROTOR HALF-SPAN WIND TUNNEL MODEL

Within the TILTAERO research program, the aerodynamic interactions between the rotor, the nacelle and the wings in different flight configurations have been studied [2], [3]. The wing consists in a fixed half-wing and a moveable half-wing allowing to limit the loss of lift due to the rotor downwash in hover. The TILTAERO rotor is based on the ERICA design [1], proposed by AGUSTA. Within the ADYN program, ONERA was responsible for the aerodynamics and acoustics optimizations for a new rotor dedicated to ERICA concept. The purpose of this activity was to perform a numerical optimization of a new set of blades (ADYN blades), starting from TILTAERO blade design. Therefore the ADYN blades were manufactured using the TILTAERO experience. Eventually, both rotors were evaluated for the aerodynamic and aero-acoustic performance on the TILTAERO mock-up in the DNW LLF in the same conditions.

1.1 ERICA mock up characteristics

The TILTAERO wind tunnel mock-up is a half-span 40% Mach-scaled model based on the advanced European tilt-rotor concept ERICA. It is constituted by three main components: the four-bladed gimbaled prop-rotor which has a diameter of 2.96m, the tiltable nacelle and the wing which has a span length of 2.22m. In order to reduce the prop-rotor download effects the wing is split into two parts: the inner wing which is fixed to a fairing representing the fuselage and the outer wing which is able to independently tilt with respect to the fixed wing and the nacelle (Figure 2).

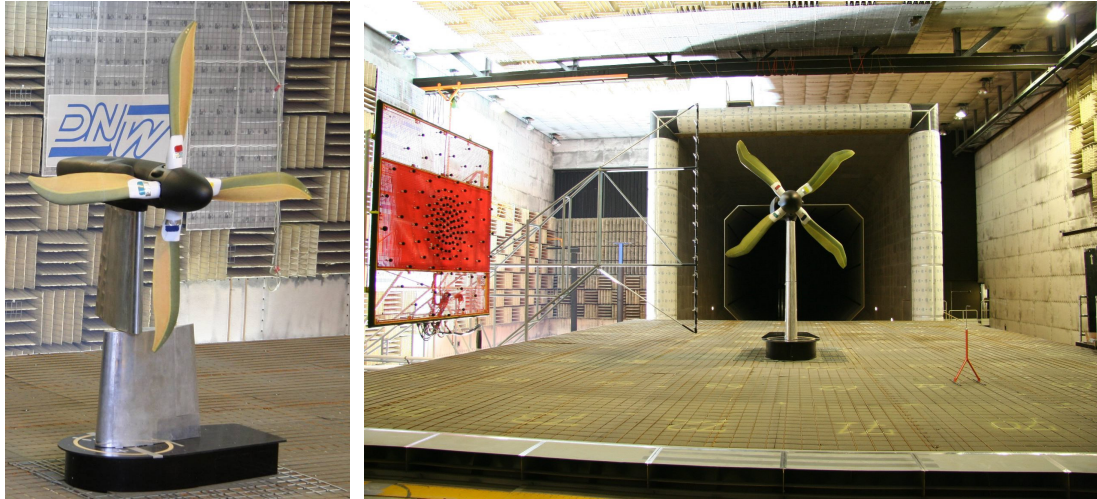


Figure 2: The TILTAERO half-span mock-up in the DNW-LLF wind tunnel (left) and aero-acoustic test set-up in the 8*6 meter $\frac{3}{4}$ open test section (right)

The mock-up was vertically mounted in the $\frac{3}{4}$ open test section of the DNW-LLF wind tunnel. The test campaign has covered a wide range of points of the flight envelope, from low speed helicopter mode to medium speed airplane mode, with the parametric variation of component settings like the wing incidence, the tilt angle, the nacelle attitude for each rotor operating point. In order to allow the phenomena investigation the model was fully instrumented. A number of unsteady pressure sensors were located along five blade sections and along three wing sections. Furthermore, the integrated loads on the prop rotor and wings were measured through balances whereas blade moments and deformations were derived from strain gauges measurements. Finally, steady pressure measurements on the wings have completed the data base.

Concerning the blades (TILTAERO and ADYN), they were both manufactured and instrumented by NLR. For each rotor, 2 blades were instrumented with strain gauges at several sections and all the blades benefits from Safety Of Flight strain gauges near the blade attachment. The ADYN rotor blades instrumentation was specified in order to get valuable unsteady pressure distribution for a detailed aero-acoustic analysis of the tests results, and as far as possible in order to be able to compare with the TILTAERO blades pressure distribution. The ADYN blades were finally equipped with 70 pressure transducers, mainly distributed in 5 sections ($r/R=0.65, 0.75, 0.8625, 0.9125$ and 0.97). Figure 3 recalls the pressure instrumentation of ADYN and TILTAERO blades. One should notice that TILTAERO differs from ADYN by having the pressure section perpendicular to the $\frac{1}{4}$ chord line and not to the feathering axis. Moreover, TILTAERO benefits from an additional inboard instrumented section at $r/R = 0.5$.

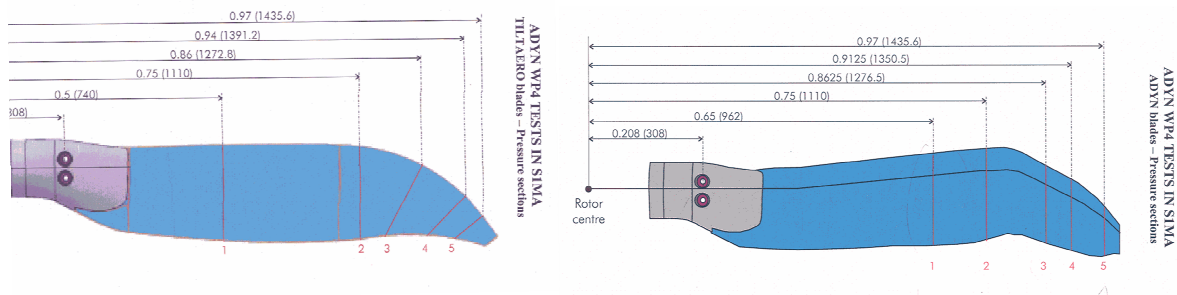


Figure 3: Recall of ADYN and TILTAERO pressure instrumentation

1.2 DNW Wind Tunnel tests

The tests took place in March 2006, in the 8x6m $\frac{3}{4}$ -open test section of the DNW-LLF, ADYN just following the TILTAERO campaign, in order to save preparation time for the model (Figure 2). Due to a drive axis failure the available effective testing time was significantly reduced. Moreover, contrary to the planned test conditions, the campaign was conducted at 80% of the full RPM rotational and free stream speed in order to avoid possible damages to the model resulting from the high vibrations observed during the preparatory phase of the test campaign.

The TILTAERO campaign dealt with the aerodynamic interactions on the wing, using the TILTAERO rotor for several configurations in the conversions corridor, from hover flight to airplane level flight. The ADYN campaign concentrated on the rotors aero-acoustic evaluation (TILTAERO rotor and the optimized ADYN rotor), performed for descent flight conditions previously selected. Furthermore, for both rotors hover measurements were done for increasing blade pitch angles.

2. NUMERICAL METHODS

The ONERA object-oriented computational code *elsA* (Ensemble Logiciel de Simulation en Aérodynamique), solves the Reynolds averaged Navier-Stokes equations in a finite volume formulation on multiblock structured meshes. The solver is used for a large variety of configurations (aircraft, turbomachinery, helicopter, tiltrotor...). Concerning aerodynamic interactions, numerical simulations of the experimental model configurations from cruise to conversion were performed at ONERA with this *elsA* software. Navier-Stokes computations were performed with a quasi-steady approach to model the rotor, using an actuator-disk. The isolated blade calculation, performed to evaluate and optimize the rotor performance in hover mode, also used a steady approach with the *elsA* code. Moreover the chimera technique with overlapping grids was used to simplify the meshes generation for both kind of calculations.

2.1 Quasi-steady approach

The numerical parameters used to calculate the rotor/wing aerodynamic interaction are based on a 2nd order Jameson scheme space discretisation with a scalar artificial viscosity including Martinelli's correction combined with a LU-SSOR scalar relaxation implicit phase with backward Euler time integration. Among the several turbulence models available in *elsA*, the Wilcox $k-\omega$ model with SST correction was used. The computations were initialised with 20 laminar iterations.

The simulation of a rotating machine (rotor, propeller...) can be simplified by modelling the rotor as a lifting surface, called "actuator disk". It represents the rotor loads which are averaged in time and applied on a surface grid in a steady flow computation. The actuator disk model is introduced into the code as a particular boundary condition where discontinuous aerodynamic quantities are prescribed. Due to the steady-state assumption, a great reduction of computational cost is achieved by comparison with an unsteady computation of the flow around rotating blades. The boundary condition formulation behaves like a usual interface and the actuator disk source terms are simply added to the residuals for the cells lying below the actuator disk surface. The source terms which model the discontinuities of the flow field are calculated by blade element theory with the HOST software allowing either a uniform global lift or variations in the radial and azimuthal directions on the disk (non-uniform actuator disk). In the present study, a uniform actuator disk has been used to perform the different test cases.

The construction of a multi-block mesh around complex geometries is difficult and needs a good know-how. The Chimera method allows simplifying the process of mesh generation by using a Cartesian background grid, on which we can overlap additional body parts, the nacelle, the two wings, the wind tunnel support and the actuator disk (Figure 4) The technique consists in introducing classical overlapping boundary conditions and also masks conditions around solid areas which will influence the overlapped grids: the nacelle, both wings, the wind tunnel support and the actuator disk in our case. Each grid may overlap several other grids.

Concerning the Cartesian background grid, a mask on the nacelle, the two wings, the wind tunnel support and the actuator disk boundary is applied. Then, the associated domains are masked and the data exchange are realised by interpolation in the vicinity of the mask. Among the several methods and parameters available to adapt the mask and interpolation to the configuration, we used the ADT method (Alternating Digital Tree) with one point outside the mask, made of Cartesian elements.

The grid was realised by ONERA with the ICEM-CFD software. The Cartesian background grid contains a total of about 1 million points distributed in 6 blocks. The nacelle 'O-grid' topology contains a total of about 3 million points distributed in 10 blocks with a first cell size of 3 microns. The fixed wing is meshed in a 'C-H' topology and has a total of about 1.4 million points distributed in 8 blocks whereas the tiltable wing has a total of about 1.3 million points distributed in 8 blocks. The wind tunnel support is meshed in a 'C-H' topology and has a total of about 500.000 points distributed in 10 blocks. The gaps between the wind tunnel support, the two half wings and the nacelle are also modelled. The actuator disk grid has a total of 150000 points distributed in 4 blocks. The computations require about $2\mu\text{s}/\text{point}/\text{iteration}$ CPU time on a NEC SX-8 computer with about 10Go memory (3000 iterations require about 14 CPU hours for a total of 7.3 million points).

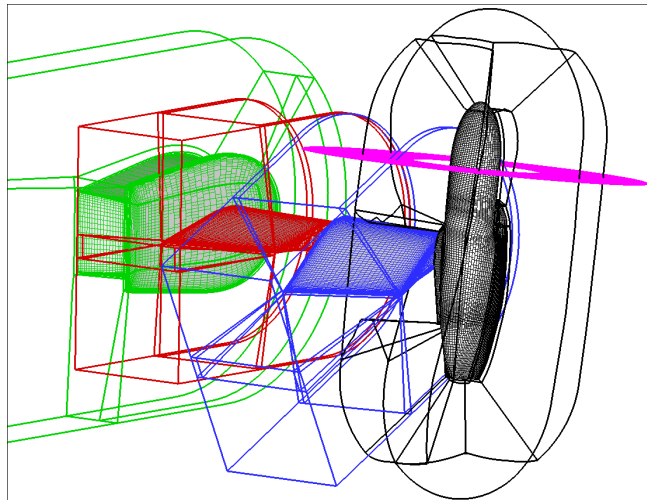


Figure 4: The TILTAERO half-span mock-up grid realised by ONERA

2.2 Isolated rotor approach

The CFD *elsA* computations were performed using the Chimera method. Actually, the CATIA definition of both blades, used to manufacture the moulds, was provided to ONERA to generate the meshes. In order to leave the possibility to integrate the nacelle mesh in future calculations, the surface definition of the blades start at $R=0.25\text{m}$, that is to say inside the cuff area, where the ADYN and TILTAERO blades are similar. It was decided to use Chimera mesh in order to be able

to perform quickly polar calculations, both in hover and in cruise flight (ADYN WP4). Moreover, the expected separated flow area at the root will be simulated (even if not completely) and its effect on the blade aerodynamic part can be represented. Figure 5 below presents the Chimera mesh of both blades and their skin mesh. The calculations were run using one blade mesh in a $\frac{1}{4}$ cylindrical background grid with periodic conditions on each side and Froude conditions on the external boundaries.

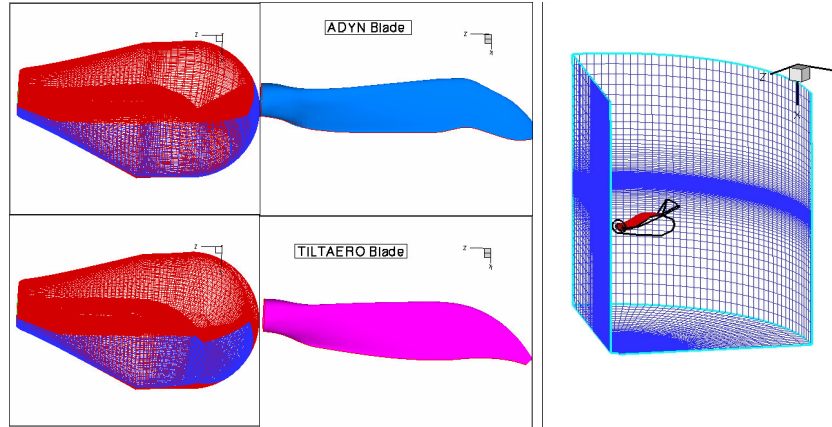


Figure 5: Chimera meshes of the blades (left) and the background grid (right)

3. RESULTS AND DISCUSSION

3.1 The conversion corridor

The conversion corridor corresponds to the tilt-rotor flight envelope containing the critical flight phase from the helicopter hover mode to the airplane level flight mode. Thus, it is very important to understand the aerodynamic interactions between the wings, the nacelle and the rotor in order to improve the aircraft performance and stability. Therefore the TILTAERO test campaign covered a wide range of the flight envelope. In particular six reference test points were chosen in the conversion corridor: the hover flight configuration, four conversion configurations from very low speed to medium speed and finally the airplane level flight configuration at medium speed. Each test points have been evaluated both by the wind tunnel tests and the numerical simulations previously described.

Test Case TP1 – Hover flight case

The model set-up for the hover flight corresponds to a nacelle tilt angle equal to 87° , a fixed wing angle of attack set to 0° while the wind speed is zero and a movable wing pitch is set to 80° . The prop rotor thrust used for the actuator disk corresponds to 5100N.

From a numerical point of view this case is the most difficult one because the wind speed is close to zero. The strategy used to perform the numerical simulation was to initialise the flow with 500 iterations at a wind speed of 10m/s which was then decreased to 1m/s and finally 0.1m/s. Figure 6 presents the convergence history of the download force on the wings for the hover case. Thanks to the ERICA concept, the loads on both wings are very small as the fixed part is not impacted by the rotor wake and the tiltable component is aligned with the rotor downwash direction. A further configuration with both wings not tilted was tested in order to confirm the gain due to the ERICA concept. In this case 600N download is obtained on the outer wing (about 12% of the rotor thrust) compare to 40N with the ERICA concept (less than 1% of the rotor thrust). In addition to the important gain of rotor thrust, the ERICA concept also provides a significant stability improvement on the outer wing loads. Figure 6 presents the iso-Mach contours on a slice in

the nacelle plane with streamlines and the pressure contour on the mock-up skin. The global view of the flow around the mock-up shows the consistency between the boundary conditions and the converged solution obtained with 0.1m/s free-stream. Vortices generated on both sides of the actuator disk and above the rotor downwash can be noted. One can notice that the vortices generated by the blades at the root might be smaller than those actually calculated with the uniform actuator disk. The pressure contours and the friction lines on the wings confirm that only the outer wing is impacted by the rotor downwash.

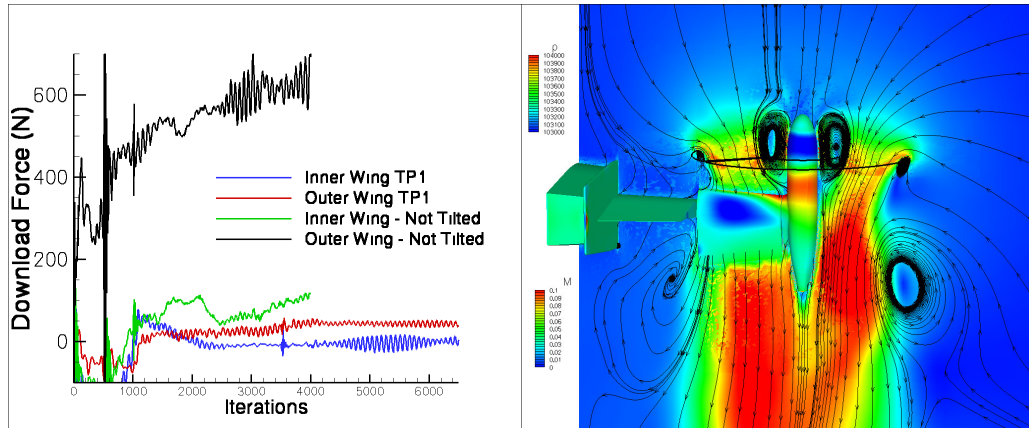


Figure 6: Time history of the download force on both wings for the hover case (left) and streamlines in the contour of Mach number and pressure distribution on the skin (right)

Test Case TP2 – First conversion case

The model set-up for the first conversion case corresponds to a nacelle tilt angle equal to 84.8° , a fixed wing angle of attack set to 2.8° and a movable wing pitch set to 29.5° . The prop rotor thrust used for the actuator disk corresponds to 5700N and the wind velocity is equal to 26.3m/s.

This case is also difficult to compute, because the speed is very low and the flow separated on the outer wing. Figure 7 presents the convergence history of the lift and drag forces for both wings and the nacelle. Even if the loads fluctuations show the instability of this configuration, the aircraft control and lift are mainly produced by the rotor at low speed. Figure 8 presents a comparison between experimental and numerical values of the normal force distribution along the wing span. The normal force level is well predicted by the simulation taking into account the weak level of lift of both wings in addition to the instability aspect of the flow especially on the outer wing. It should be noticed that the experimental values correspond to steady pressure measurements whereas the numerical ones correspond to a flow field post-treatment at a given time. Figure 8 presents the Mach contours on a slice in the nacelle plane with streamlines and the pressure contours on the mock-up skin. The global view of the flow around the mock-up shows the important flow separation on the outer wing. It appears that the rotor downwash has been over-estimated and is not sufficient to reattach the flow on the outer wing. The adaptation of the outer wing angle of attack could be a solution to reduce the flow separation and the loads instability. Numerical simulations of different angles of attack could allow optimising the corridor conversion configuration which is critical in terms of aircraft stability.

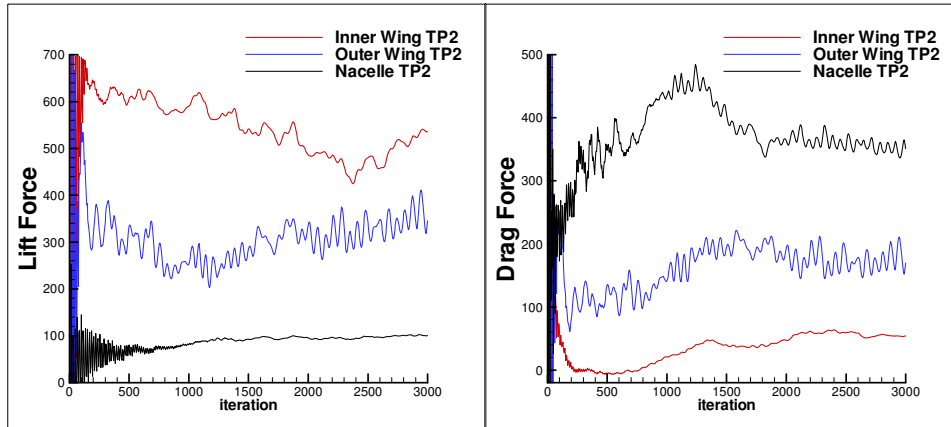


Figure 7: Time history of the lift and drag force on both wings and nacelle for the TP2 case

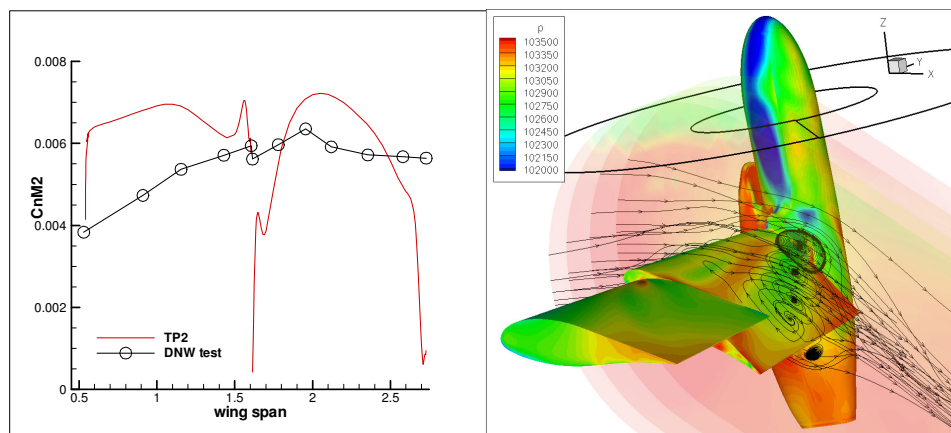


Figure 8: Experimental and numerical normal force along the wingspan (left) and streamlines in slices normal to the outer wing and pressure distribution on the skin for the TP2 case (right)

Test Case TP3 – Second conversion case

The model set-up for the second conversion case corresponds to a nacelle tilt angle equal to 74.9° , a fixed wing angle of attack set to 3° and a movable wing pitch set to 10.7° . The prop rotor thrust used for the actuator disk corresponds to 4600N and the wind velocity is equal to 42.88m/s.

Figure 9 presents the convergence history of the lift and drag forces for both wings and the nacelle. Even if the loads fluctuations show the instability of this configuration, it is fairly reduced compared to the previous case because the free-stream velocity and loads are larger. One can notice that the inner wing ensure a reasonable part of the lift whereas the nacelle produces a significant drag force. Figure 10 presents a comparison between experimental and numerical values of the normal force distribution along the wing span. The normal force distribution is well predicted by the simulation taking into account the flow separation on the outer wing. But the level is slightly overestimated by the simulation for the attached flow especially on the inner wing. It can be noted that the flow separation on the outer wing generates a very important loss of lift. Figure 11 presents a comparison of the experimental and numerical pressure coefficient on both wings normal sections (A, C, D, F, H noticed on Figure 10). Concerning the inner wing, the normal force underestimation is confirmed and could be explained by a slight angle of attack increase in the test, since no wind tunnel correction was applied on the experimental result. Regarding the outer wing, the pressure coefficients are quite well estimated on the three sections, especially on the section H which is fully

separated in both experiment and simulation. Finally, the global view of the flow around the mock-up shows the reduction of the flow separation on the outer wing near the nacelle (Figure 10).

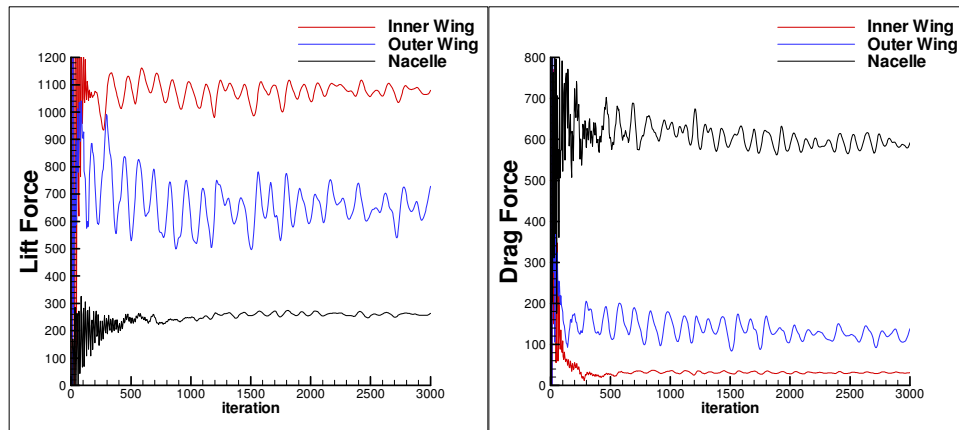


Figure 9: Time history of the lift and drag force on both wings and nacelle for the TP3 case

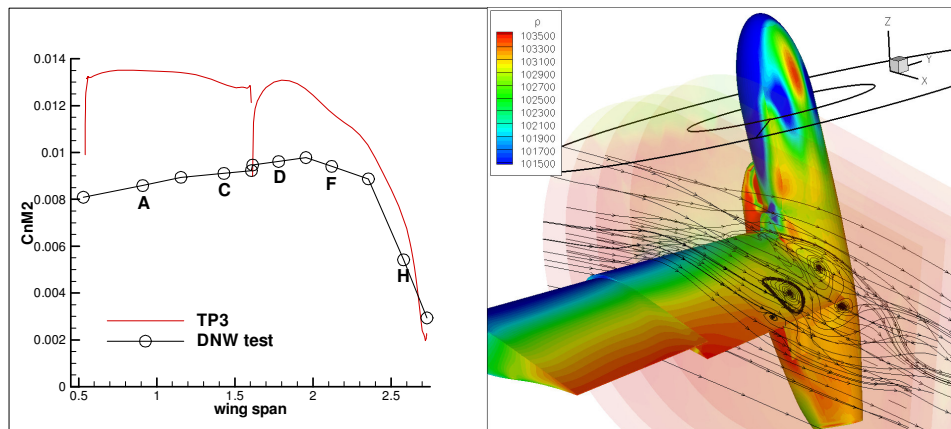


Figure 10: Experimental and numerical normal force along the wingspan (left) and streamlines in slices normal to the outer wing and pressure distribution on the skin for the TP3 case (right)

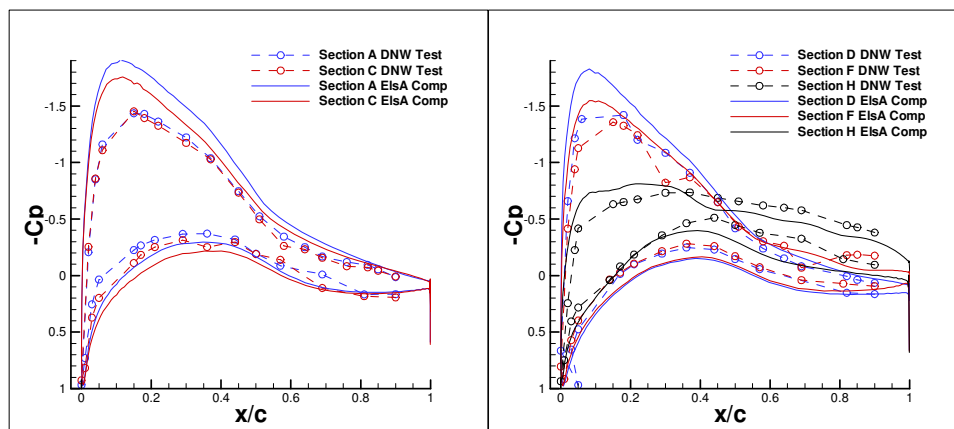


Figure 11: Experimental and numerical pressure coefficient on the inner wing (left) and on the outer wing for the TP3 case (right)

Test Case TP4 – Third conversion case

The model set-up for the third conversion case corresponds to a nacelle tilt angle equal to 60° , a fixed wing angle of attack set to 3° and a movable wing pitch set to 3.7° . The prop rotor thrust used for the actuator disk corresponds to 3700N and the wind velocity is equal to 57.1m/s.

The small loads fluctuations show that this case is more stable than the previous ones because the free stream velocity is now high enough and both wings angles of attack very small (Figure 12). One can notice that the inner wing ensures 60% of the wings lift whereas the nacelle produces about 80% of the total drag force. The normal force distribution is very well predicted by the simulation even if the level is still overestimated by the simulation (Figure 13). I can be noted that the separation and the loss of lift are together slightly reduced compared to the previous cases. A slight angle of attack increase in the experiment is still a possible reason for the pressure peak underestimation (Figure 14). At low angle of attack a slight variation of incidence is very influent on the pressure coefficient. Concerning the outer wing, the pressure coefficients are also well estimated taking into account the fact that the simulated pressure coefficient on section H corresponds to an instantaneous post-treatment. Finally, the global view of the flow around the mock-up shows the reduction of the flow separation on the outer wing near the nacelle (Figure 13).

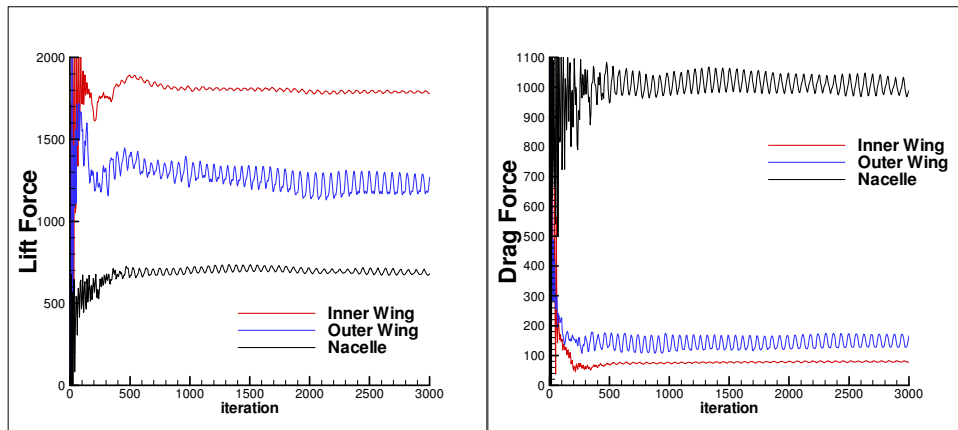


Figure 12: Time history of the lift and drag force on both wings and nacelle for the TP4 case

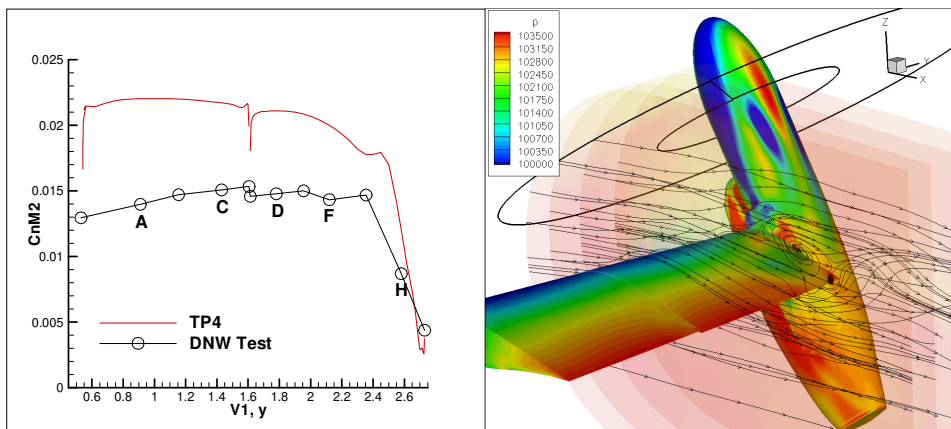


Figure 13: Experimental and numerical normal force along the wingspan (left) and streamlines in slices normal to the outer wing and pressure distribution on the skin for the TP4 case (right)

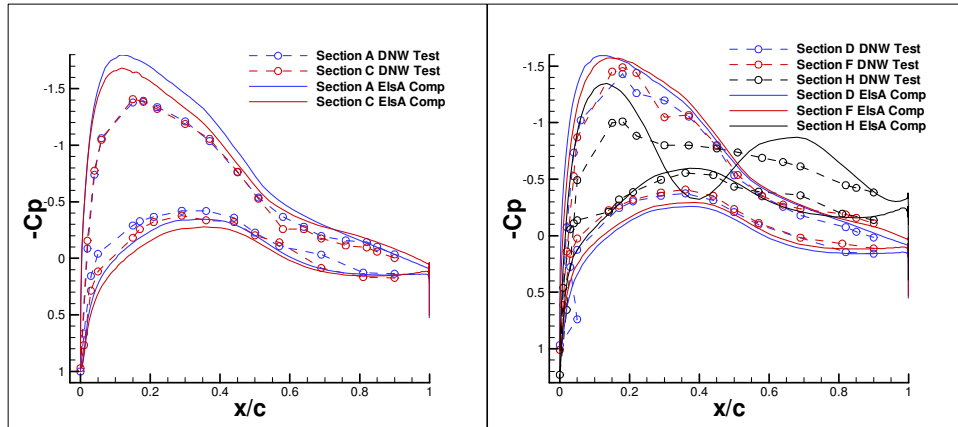


Figure 14: Experimental and numerical pressure coefficient on the inner wing (left) and on the outer wing for the TP4 case (right)

Test Case TP5 – Last conversion case

The model set-up for the last conversion case corresponds to a nacelle tilt angle equal to 45° , a fixed wing angle of attack set to 3° and a movable wing pitch set to 3.2° . The prop rotor thrust used for the actuator disk corresponds to 2600N and the wind velocity is equal to 63.3m/s.

This case is the last configuration before level flight (Figure 15). The loads fluctuations show that this case is even less stable than the previous one because the nacelle-wing junction which is similar to an airfoil shape has an angle of attack of 45° . This junction generates important flow perturbations and contributes to the large nacelle drag force corresponding to about 75% of the total drag force. The normal force distribution is very well predicted by the simulation even if the level is still overestimated without the wind tunnel wall correction (Figure 16). Concerning the pressure coefficient, the prediction is very good on both wings but the small angle of attack difference is obviously noticeable (Figure 17). Finally, the global view of the flow around the mock-up clearly shows the effect of the nacelle-wing junction on the outer wing skin pressure distribution (Figure 16).

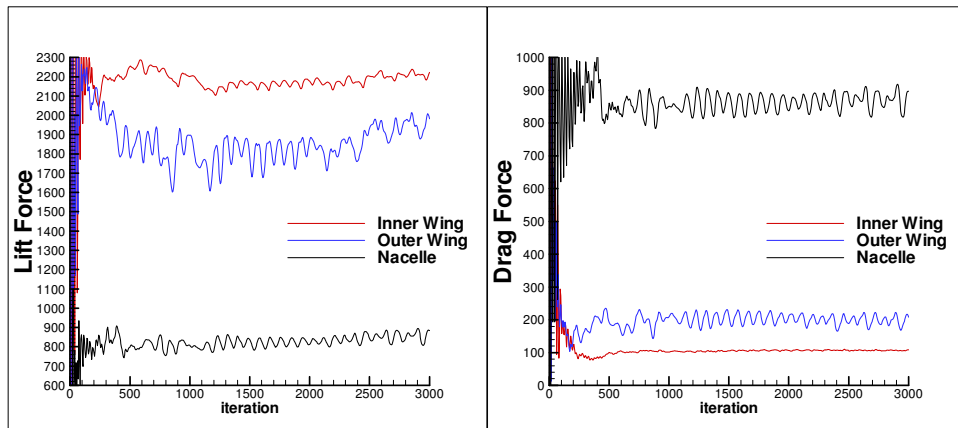


Figure 15: Time history of the lift and drag force on both wings and nacelle for the TP5 case

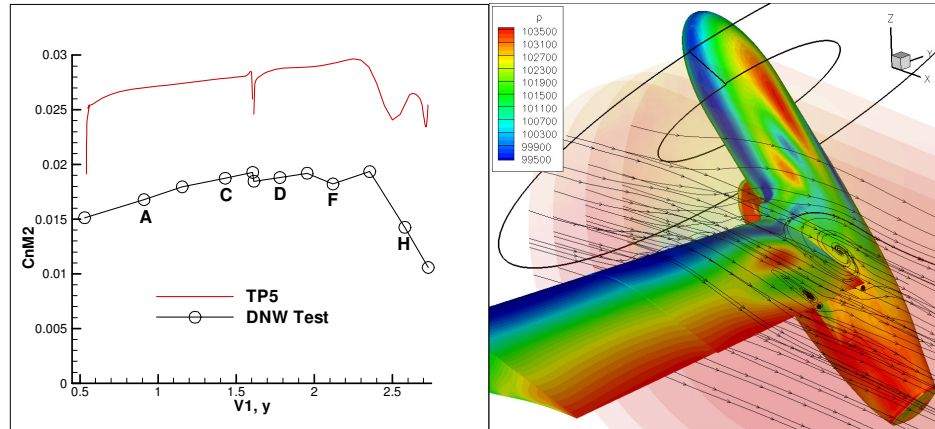


Figure 16: Experimental and numerical normal force along the wingspan (left) and streamlines in slices normal to the outer wing and pressure distribution on the skin for the TP5 case (right)

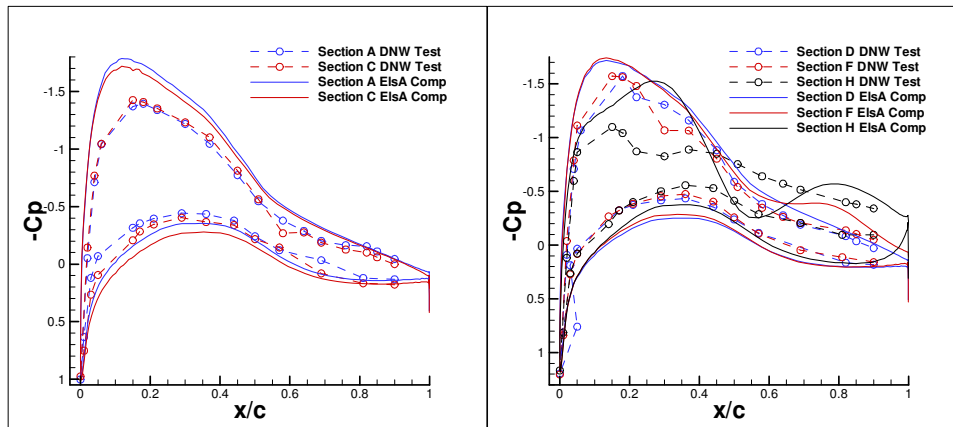


Figure 17: Experimental and numerical pressure coefficient on the inner wing (left) and on the outer wing for the TP5 case (right)

Test Case TP7 – Level flight case

The model set-up for the level flight case corresponds to a nacelle tilt angle equal to 0.3° , a fixed wing angle of attack set to 3.3° and a movable wing pitch set to 3.3° . The prop rotor thrust used for the actuator disk corresponds to 800N and the wind velocity is equal to 57.4m/s.

This case is the aircraft configuration in medium speed level flight. The lift force history presented on Figure 18 shows that it is a very stable case. There is no separation on the wings and the numerical results are reliable. The normal force distribution is very well reproduced by the simulation even if the level is still overestimated without the wind tunnel wall correction (Figure 18). This is confirmed by the pressure coefficient which prediction shape is quite well predicted on both wings (Figure 19).

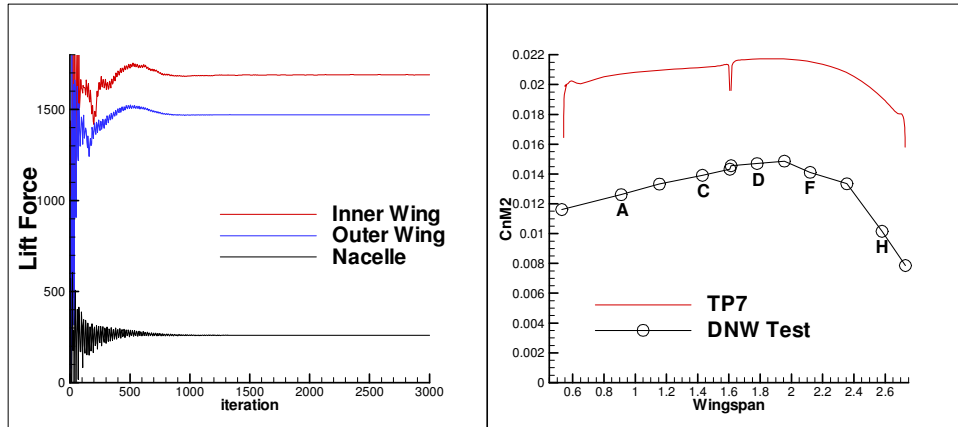


Figure 18: Time history of the lift force on both wings and nacelle (left) and experimental and numerical normal force along the wingspan for the TP7 case (right)

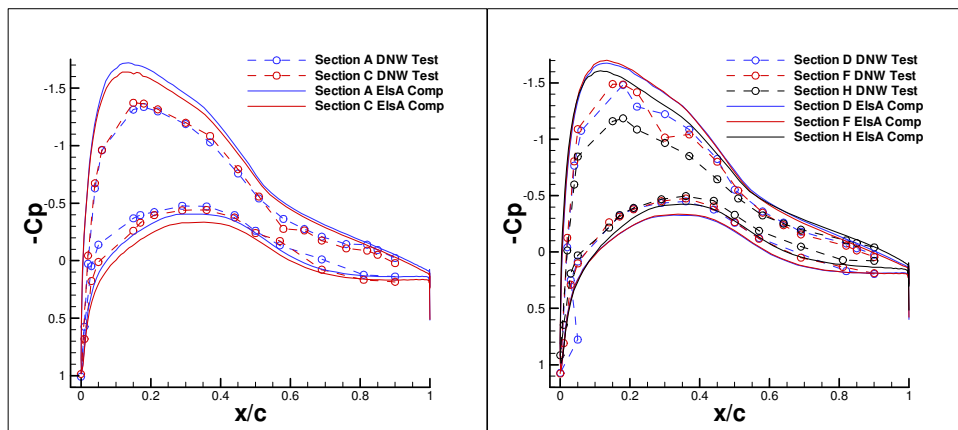


Figure 19: Experimental and numerical pressure coefficient on the inner wing (left) and on the outer wing for the TP7 case (right)

3.2 The rotor performance

In the frame of the ADYN and DART projects, ONERA was responsible for the aerodynamic and acoustic optimizations for a new rotor dedicated to the ERICA concept. The purpose of this task was to experimentally evaluate the ERICA reference blades (TILTAERO blades) in terms of noise characteristics and to perform a numerical optimization of a new set of blades (ADYN blades), which will be designed, manufactured and tested in the same conditions.

3.2.1 ADYN rotor optimization

The specifications and constraints for the numerical optimization were specified early in the project [4] and are the following. First, an acoustic objective with a noise level lower by 4dB than the reference TILTAERO blade in Flyover and Take-off mode, and lower by 6dB than the reference in Landing mode. Then, good performance both in hover and cruise were required following the general characteristics of the ERICA 4 bladed rotor, with Hover performance ($FM > 0.86$ for $Ct/\sigma = 0.116$), cruise performance ($\eta > 0.87$ for $Ct/\sigma = 0.072$ at $V = 350 \text{ kt}$ at 7500 m) and maximum lift capability ($Ct/\sigma_{\text{max}} = 0.191$ for $70 < V < 90$).

The list of elements which can be modified for the optimization was also agreed from the beginning: blade planform, chord distribution, twist law, mean chord, sweep, anhedral. The

activities were done in parallel to the DART project, because it was clear from the specifications that the ADYN aero-acoustic optimization had to account for the DART aerodynamic optimization. After many parametric studies done by different partners using different aero-acoustic computational tools, the so-called ADYN OPT2D15-3 blade was selected as the ADYN optimized blade (Figure 20). The main reasons for this selection were first that the blade showed lower radiated noise levels compared to the ADYN reference blade (close to TILTAERO) for most flight conditions (-3dB as an average), despite higher levels for some specific conditions (2dB at 10° descent flight); furthermore the blade had very good hover and cruise performance, always better than TILTAERO.

The definition of the ADYN blade structural characteristics was then performed, starting from the structural properties of the OPT2D15 blade based on DART technological studies and using the TILTAERO blade experience. A specific technological study was performed for the ADYN blade manufacturing. The main objective of this technological study was to match the nominal Mach scaled values of the inertial and structural properties of the blade, considering a real manufacturing procedure and with respect to a set of available experimental data of the characteristics of the materials employed for the blade manufacturing.

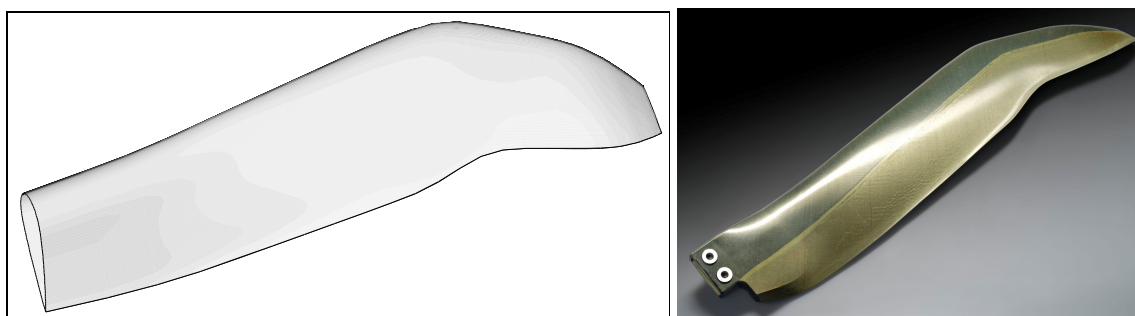


Figure 20: The ADYN optimized blade: design (left) and manufactured (right)

3.2.2 Hover tests

The hover tests were performed in the DNW, with the TILTAERO set-up. One polar was made for the TILTAERO rotor and 2 polars were performed for ADYN blades. The tests were repeated with the stubs.

Global performance

Figure 21 presents the comparison of the figure of merit (FM) versus thrust obtained from the DNW measurements and *elsA* calculations. The figure of merit (FM) obtained from the DNW measurements clearly indicates that the ADYN optimized rotor reaches higher performance than the TILTAERO rotor, and also reaches its maximum FM for much higher thrust values. One can notice that the ADYN FM_{max} is 5 counts higher than the TILTAERO one and that this value is obtained for a thrust coefficient 30 % higher. Concerning the computational results, one can check the quite good agreement between CFD and experiment for the rotors can be checked, that is to say both the maximum FM and the thrust for which it is obtained are in line with experimental results. Moreover the TILTAERO sudden loss of FM is afterwards well predicted by CFD.

Figure 22 presents a comparison, in terms of skin friction lines, on the upper side of the 2 blades for a thrust coefficient close to $C_t/\sigma = 0.12$ (0.11 for TILTAERO and 0.125 for ADYN). For all blades, a zone of separated flow can be identified at the blade trailing edge in the root area. This is the consequence of the high thickness of the blade root. Another zone of separated flow can also be observed at the blade tip but its extension is clearly different between the blades. On the ADYN

blade, only the last percent of the blade shows a separated flow. But, for TILTAERO blade, the zone of separated flow increases significantly representing more than the 5 last percent of the blade thus explaining the difference of FM between the 2 rotors and the drop of for the TILTAERO blade FM.

Then, a visualization of the vortical structures emitted by the 2 blades for the same configurations ($Ct/\sigma \approx 0.11$) is proposed in Figure 22. The vortex of the preceding blade is clearly visible. It seems clear that the separated area responsible for the loss of FM is due to the passage of the vortex of the preceding blade in the TITLAERO case whereas, even for a higher thrust, the ADYN blade is less impacted.

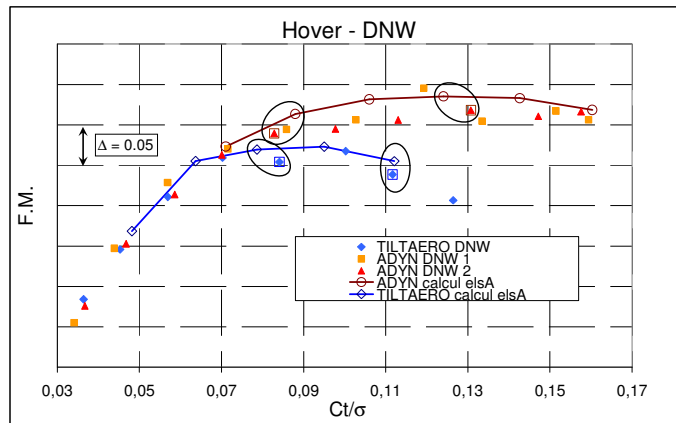


Figure 21: Hover performance (DNW tests)

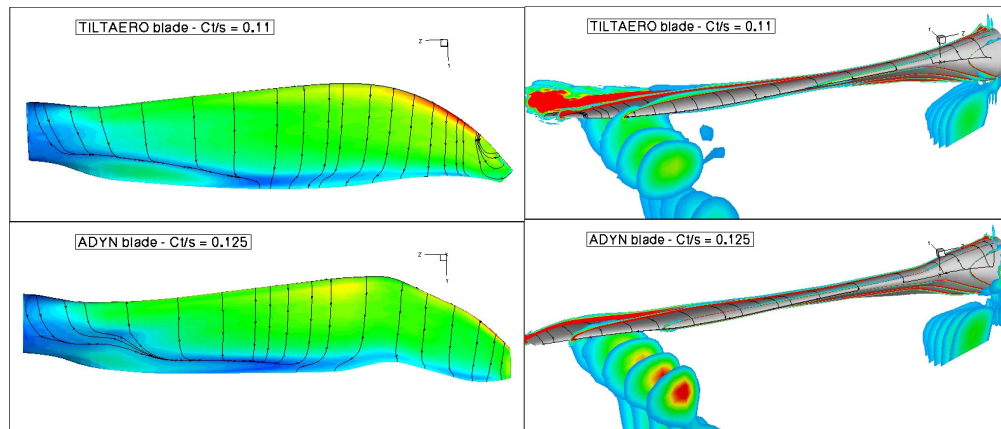


Figure 22: Skin friction lines at $Ct/\sigma \approx 0.1$ (left) and vortical structures emitted by the 2 blades at $Ct/\sigma \approx 0.1$ (right)

Local pressure comparison

The aim of this paragraph is to check the accuracy of the CFD calculations for the local behavior of the blades, using the experimental pressure information. Figure 21 recalls the hover performance curve measured on the DNW where the experimental configurations selected for comparisons with CFD are enlightened. Concerning the TILTAERO rotor, 2 configurations were retained, one close to FMmax around $Ct/\sigma = 0.08$, and the other at stall (last measured point). Regarding the ADYN rotor, 2 configurations were also retained, one at the same Ct/σ as the TILTAERO FMmax and the other one at the ADYN FMmax, close to $Ct/\sigma = 0.13$.

Figure 23 presents the experimental and the calculated pressure distribution for the ADYN and TILTAERO blades at the same spanwise location. Both rotors have similar experimental thrust (close to Ct/σ close to 0.08). One has to note that some kulites are defective, especially for the TILTAERO rotor. Actually, most of the TILTAERO leading edge sensors didn't work during the ADYN tests. The ADYN kulites appear to be less defective. Thus there is not enough reliable kulites on TILTAERO to compare with the CFD calculation even if, for section C for example, the agreement seems rather satisfactory. The comparison for the ADYN blade is more interesting with a good agreement in the first 50 % of chord, on the suction side for all 4 instrumented sections.

Figure 24 presents the experimental and the calculated pressure distribution for the ADYN and TILTAERO blades for the second retained configuration. Here, the ADYN rotor has a higher experimental thrust than TILTAERO. The low number of reliable kulites on TILTAERO is here also limiting the comparison. For section E, for example the CFD calculation predicts an area of separated flow near the leading edge that can not be fully confirmed by the experimental data, due to the lack of kulites information in this region. For the ADYN blade, the agreement between CFD and experiment remains acceptable even for section E where no area of separated flow can be suspected.

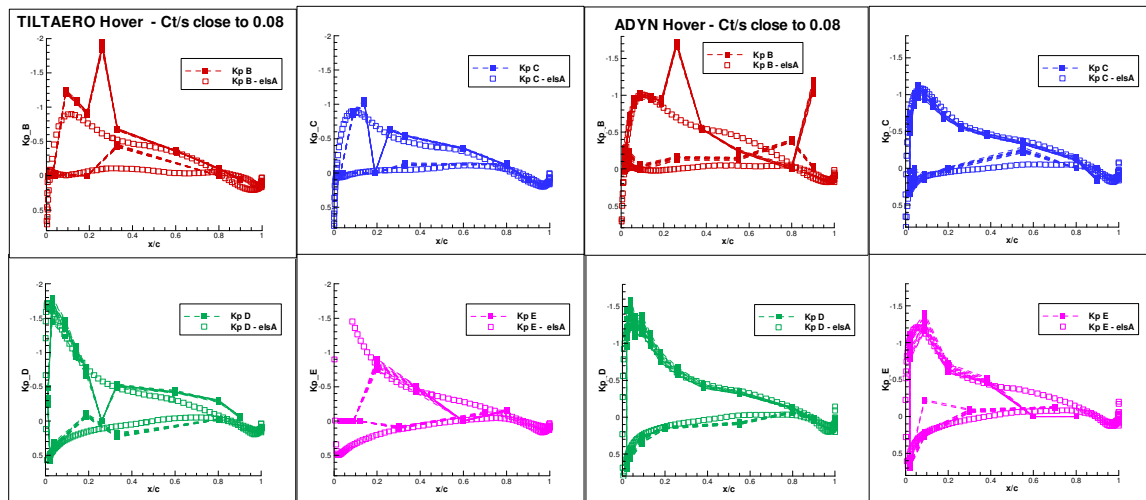


Figure 23: comparison of experimental and calculated K_p distribution for ADYN and TILTAERO blade (Ct/σ close to 0.08)

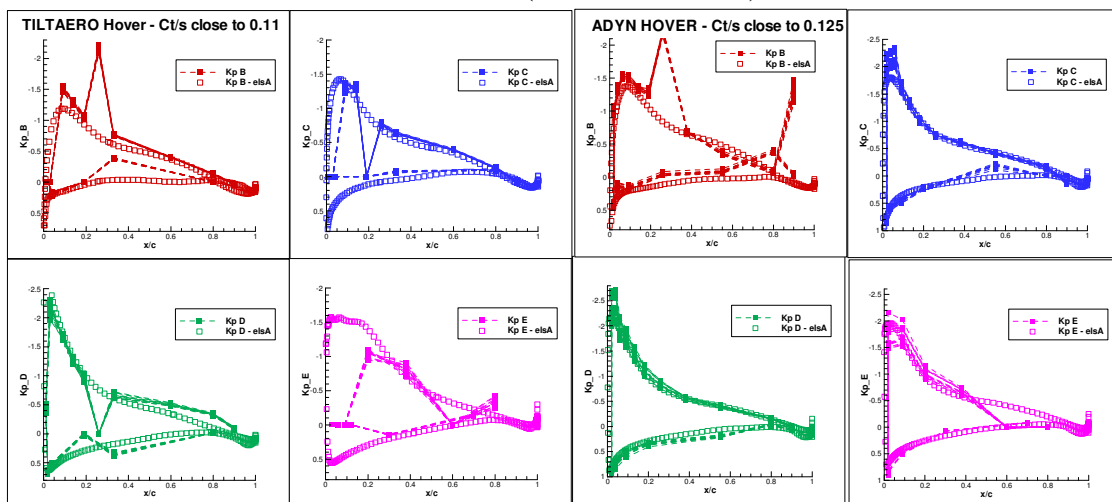


Figure 24: comparison of experimental and calculated K_p distribution for ADYN and TILTAERO blade (Ct/σ close to 0.11)

4. CONCLUSION

Within the frame of European programs on tilt-rotors, ONERA has participated in the evaluation of a tilt-rotor aerodynamic interaction study and a rotor aero-acoustic performance optimization. Experimental measurements were conducted in the 8x6m $\frac{3}{4}$ open test section of the DNW-LLF wind tunnel on the half-span 40% Mach-scaled model based on the advanced European tilt-rotor concept ERICA. Several test points in the conversion corridor have been measured with the TILTAERO blades and a comparative study has been done with the aero-acoustic optimized ADYN blades in hover and descent flight.

Concerning the numerical point of view, ONERA used the *elsA* software to perform Navier-Stokes quasi-steady simulations of the complete TILTAERO half-span model. Several methods, such as chimera grids or actuator disk, have been used to simplify those computations and make it possible to simulate all the chosen test cases in the conversion corridor, from hover to level flight. Regarding the isolated rotor, advanced numerical methods have also been employed to perform high quality simulations allowing to achieve the aero-acoustic performance optimization.

The conversion corridor is the most critical phase of the tilt-rotor flight and the aerodynamic interactions between the rotor, the wings and the nacelle have been studied within the TILTAERO European program. These strong aerodynamic interactions appear more especially between the nacelle-wing junction and the flow separation of the outer wing which were obtained for the different flight configurations from very low speed to the last conversion case. Moreover, detailed comparison between numerical and experimental result allows us to be quite confident in the numerical simulation of the tilt-rotor conversion flight, taking into account the fact that there were no wind tunnel corrections during the test. Finally, as we are now capable to understand and predict these difficult interaction phenomena during the conversion phase, some improvements of the ERICA design can be performed by optimising this wing-nacelle junction in order to limit the important loss of lift due to the outer wing flow separation, in addition to the nacelle drag reduction.

The rotor optimization activities carried out in those European programs led to the design of an innovative tilt-rotor equipped with the ADYN blades. Wind-tunnel tests proved the very good hover efficiency of the ADYN blades compared to the TILTAERO blades. Moreover, the optimization was performed mainly with CFD computations (both *elsA* and *FLOWer*) and they managed to predict the performance of the rotors with a good accuracy. A good confidence can therefore be expected from CFD tools on the design of 3D blades of tilt-rotor or helicopters, at least for hover conditions.

Finally this paper constitutes a status on the ONERA know-how about tilt-rotor aerodynamic interactions and rotor performance optimization, in terms of experimental measurement on half-span model and rotor in addition to advanced numerical simulations of complete tilt-rotor interactions or isolated rotor aero-acoustic performance. The ONERA involvement in tilt rotor aerodynamics is being pursued within the new NICETRIP European project.

ACKNOWLEDGMENT

The authors would like to gratefully thank all the partners of those different European programs on tilt-rotor (TILTAERO, DART and ADYN) and especially the European Union for partly funding those studies under the Competitive and Sustainable Growth Program in the 5th Framework.

REFERENCES

- [1] F. Nannoni, G. Giancamilli, M. Cicalè, “*ERICA: The European Advanced Tiltrotor*”, 27th European Rotorcraft Forum, Moscow (Russia), September 11-14, 2001
- [2] Visingardi, A., Khier, W., Decours J., “*The Blind-test activity of TILTAERO project for the numerical aerodynamic investigation of a tilt-rotor*”, IV Eccomas Congress, Jyväskylä, SU, July 2004.
- [3] Visingardi, A., Khier, W., Decours J., Voutsinas S. “*Code to code comparisons for blind test activity of the TILTAERO project*”, 31st European Rotorcraft Forum, Firenze, Italy, September 2005
- [4] Lefebvre T., Beaumier P., Canard S., Pisoni A., Pagano A., van der Wall B. , D’Alascio A., Arzoumanian C., Riziotis V and Hermans C., “*Aerodynamic and aero acoustic optimization of modern tilt-rotor blades within the ADYN project*”, IV Eccomas Congress, Jyväskylä, SU, July 2004
- [5] P. Beaumier, Y. Delrieux, “*Description and validation of the ONERA computational method for the prediction of blade-vortex interaction noise*”, 29th European Rotorcraft Forum, Friedrichshafen (Allemagne), September 16-18, 2003